Doi: 10.1007/s11589-009-0197-9

A numerical study of comparison of two one-state-variable, rate- and state-dependent friction evolution laws*

Jeen-Hwa Wang♣

Institute of Earth Sciences, *Academia Sinica*, *P.O. Box* 1-55, *Nangang*, *Taipei*, *China*

Abstract The two one-state-variable, rate- and state-dependent friction laws, i.e., the slip and slowness laws, are compared on the basis of dynamical behavior of a one-degree-of-freedom spring-slider model through numerical simulations. Results show that two (normalized) model parameters, i.e., Δ (the normalized characteristic slip distance) and $\beta-\alpha$ (the difference in two normalized parameters of friction laws), control the solutions. From given values of Δ, β, and α, for the slowness laws, the solution exists and the unique non-zero fixed point is stable when $\Delta>(\beta-\alpha)$, yet not when $\Delta<(\beta-\alpha)$. For the slip law, the solution exists for large ranges of model parameters and the number and stability of the non-zero fixed points change from one case to another. Results suggest that the slip law is more appropriate for controlling earthquake dynamics than the slowness law.

Key words: **one-state-variable; rate- and state-dependent friction law; direct effect; evolution effect; characteristic slip displacement**

CLC number: P315.8 **Document code**: A

1 Introduction

Friction is an important factor in controlling earthquake ruptures. Laboratory experiments show two effects affecting the friction strength: direct and evolution effects (Dieterich, 1978, 1979; Ruina, 1983). The direct effect shows an instantaneous change of friction strength with a change in velocity, while the evolution effect evolves with slip following a change in velocity. Unstable slip in rock can result only when the final frictional strength is smaller than the original one. This leads to the so-called velocity-weakening process. The one-state-variable slip and slowness laws proposed by Dieterich (1978, 1979) and Ruina (1983) have been used to describe the state-dependent evolution effect. Perrin et al (1995) proposed a different friction law to describe the evolution process. However, since Nakatani (2001) assumed that Perrin's law cannot be appropriate to describe the observations, and thus will not be taken into account in this study.

Some authors compared the two laws based on the quasi-static approach. Dieterich (1992) suggested that the two laws yield similar results for most cases. Rice and Ben-zion (1996) found that the slip law leads to periodically repeated events, while the slowness one allows apparently chaotic sequences of large events. Roy and Marone (1996) stated that pre-seismic slip is larger for the slowness law than for the slip law. Nakatani (2001) addressed that the slip law is more appropriate than the slowness law to interpret his experimental results.

On the basis of a dynamic approach, He et al (2003) obtained several important conclusions. ① The overall stress drops for the two laws are linearly related to the logarithm of the loading velocity through the velocity-weakening parameter "$b-a$" and the normal stress. ② The slowness law results in relatively larger peak stresses, larger quasi-static stress drop, and larger effective fracture energy than the slip law. ③ The choice of the two laws can affect the partitioning of stress drop between quasi-static and dynamic slips, as well as dynamic overshoot and strength recovery.

Based on a dynamical one-degree-of-freedom spring-slider model (abbreviated as 1DF model hereafter), Rice and Ruina (1983) found that $d\sigma^{ss}/dv<0$, where

* **Received** 11 September 2008; **accepted in revised form** 22 December 2008; **published** 10 April 2009.

♣ **Corresponding author. e-mail**: jhwang@earth.sinica.edu.tw

σ^{ss} is the steady-state stress and v is the velocity, is a necessary and sufficient condition for instability to be possible with some spring constants. Rice (1983) comprehensively studied linear and nonlinear stability conditions of the system, subjected to different friction laws. Rice and Ruina (1983) and Horowitz and Ruina (1989) pointed out the existence of a stable limit cycle for a particular choice of the parameters of the system. Gu et al (1984) claimed that when the slip law is used, instability occurs whatever choice of the parameters and a stable limit cycle never occurs. This shows a difference between the quasi-static and dynamic models. Belardinelli and Belardinelli (1996) stressed that this difference reduces the validity of the quasi-static model as an approximation of the dynamic one. Wang (2002) compared the stability conditions of the two friction laws based on a 1DF model. He found that at low velocities the stability criteria for the two laws are equal and similar to the steady-state one deduced by Ruina (1983). But, at high velocities the stability criterion for the slip law depends not only on the parameters of the friction law but also on the sliding velocity and state variable; while for the slowness law the stability criterion at high velocities is the same as that at low velocities.

The present study will compare the two one-state-variable evolution laws based on dynamical behavior of a 1DF model using the phase portrait (Thompson and Stewart, 1986). Since the system is nonlinear, numerical simulation will be performed.

2 Brief description of the model

Ruina (1983) assumed the friction strength, μ, to be described by the following one-state-variable, rate- and state-dependent function:

$$\mu = \mu_0 + b\ln\frac{\theta v_0}{D_c} + a\ln\frac{v}{v_0}, \tag{1}$$

where θ is the state variable, v is the sliding velocity, v_0 is the reference velocity and usually considered to be a constant, and D_c is the characteristic slip distance. Contributions to the total friction strength is scaled by a for the direct effect and b for the evolution one. The three parameters a, b, and D_c for some rocks were determined experimentally (Marone, 1998). Although μ is often thought to be a "strength" in the classical sense, Nakatani (2001) stressed that it must be a shear stress, σ_t, applied to the frictional interface, normalized by the normal stress, σ_n. He regarded $\mu_0+b\ln(\theta v_0/D_c)$ as an extension of the conventional frictional strength in the classical sense and named it the "interface strength" which is μ_0 when $v=v_0$ and $\theta=D_c/v_0$.

Two friction laws are commonly used to describe the state-dependent evolution effect (Marone, 1998). One is the slip law, i.e., $\mathrm{d}\theta/\mathrm{d}t = -(\theta v/D_c)\ln(\theta v/D_c)$. When $v\to 0$, $\mathrm{d}\theta/\mathrm{d}t \fallingdotseq 0$ using the l'Hospital's theorem. This indicates that no evolution occurs at $v=0$. The other is slowness law, i.e., $\mathrm{d}\theta/\mathrm{d}t = 1-\theta v/D_c$. This equation shows $\theta=D_c/v$, when $\mathrm{d}\theta/\mathrm{d}t=0$. For the two laws, the steady-state friction strength, μ^{ss}, when $\mathrm{d}\theta/\mathrm{d}t=0$, is $\mu_0+(a-b)\ln(v/v_0)$. This leads to that $\mu^{ss}=\mu_0$ at $v=v_0$. The commonly used stability criterion is $D_c>D_0(\beta-\alpha)$ (Ruina, 1983) which only depends on the parameters of the friction law. The parameters α and β are $\alpha=a/\mu_0$ and $\beta=b/\mu_0$, respectively. Based on a 1DF model, Wang (2002) concluded that at low velocities, the stability criteria for the two laws are equal and has Ruina's form. At high velocities the stability criterion is $D_c>D_0(b-a)$ for the slowness law and $-1+\ln D_c < \ln(v\theta) < -1+\ln D_c+\mu_0 D_c/D_0(b-a)$ for the slip law. In addition to D_c, D_0, and $b-a$, the latter also depends on μ_0, v, and θ. The range of stable regime increases with D_c, yet decreases either with increasing D_0 or with increasing $b-a$.

The 1DF model (see Figure 1) consists of a slider of mass, m, linked by a spring with stiffness of K. The location of the slider is u, measured from its initial equilibrium position, along the horizontal axis. The slider is loaded by a driving force with a velocity of v_p and also subjected to a rate- and state-dependent frictional force, $F(\theta, v)$, where $v=\mathrm{d}u/\mathrm{d}t$. The equation of motion of the system is

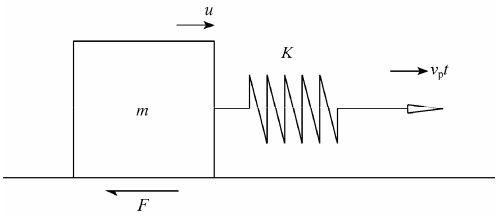

Figure 1 A dynamical one-degree-of-freedom spring-slider model.

$$m\frac{\mathrm{d}^2u}{\mathrm{d}t^2} = -K(u-v_p t) - F(\theta, v). \tag{2}$$

Let $F(\theta, v)$ be $\mu\sigma_n A$ where A is the bottom area of the slider, and thus $F(\theta, v)=\sigma_n A[\mu_0+a\ln(v/v_0)+b\ln(\theta v_0/D_c)]$. Let $F_0=\mu_0\sigma_n A$, $\alpha=a/\mu_0$, and $\beta=b/\mu_0$. This gives $F(\theta, v)=F_0[1+\alpha\ln(v/v_0)+\beta\ln(\theta v_0/D_c)]$. Substitution of $F(\theta, v)$ into

equation (2) leads to

$$m\frac{\mathrm{d}^2u}{\mathrm{d}t^2}=-K(u-v_{\mathrm{p}}t)-F_0\left(1+\alpha\ln\frac{v}{v_0}+\beta\ln\frac{\theta v_0}{D_{\mathrm{c}}}\right). \quad (3)$$

From the original definition of the model, the slider initially rests in an equilibrium state, with v=0. From the rate- and state-dependent frictional force, Nakatani (2001) rewrote equation (1) as

$$v(\sigma_{\mathrm{t}},\Psi)=v_0\exp\left\{\left[\frac{\sigma_{\mathrm{t}}}{\sigma_{\mathrm{n}}}-(\mu_0+\Psi)\right]\cdot\frac{1}{a}\right\}, \quad (4)$$

where $\Psi=b\ln(\theta v_0/D_{\mathrm{c}})$. When $\Psi\to\infty$, v=0. Equation (4) gives $v<<v_0$ when $\sigma_{\mathrm{t}}/\sigma_{\mathrm{n}}<(\mu_0+\Psi)$ and an abrupt increase in v when $\sigma_{\mathrm{t}}/\sigma_{\mathrm{n}}>(\mu_0+\Psi)$. Hence, initially the slider moves very slowly, because the applied force is less than the interface strength.

To simplify the problem, equation (3) is normalized by $\omega_0=(K/m)^{1/2}$ and $D_0=F_0/K$. The former is the frequency of oscillation of the system in the absence of friction and shows the inertial effect, while the latter is the maximum displacement of the slider exerted by F_0. D_0 and ω_0 are significant units to scale the spatial coordinate and time, respectively. The definitions of $U=u/D_0$ and $\tau=\omega_0 t$ lead to $\mathrm{d}u/\mathrm{d}t=[F_0/(mK)^{1/2}]\mathrm{d}U/\mathrm{d}\tau$, $\mathrm{d}^2u/\mathrm{d}t^2=(F_0/m)\mathrm{d}^2U/\mathrm{d}\tau^2$, and $\upsilon=\mathrm{d}U/\mathrm{d}\tau$. Define $\upsilon=v/D_0\omega_0$, $\Theta=\omega_0\theta$, $\upsilon_{\mathrm{p}}=v_{\mathrm{p}}/D_0\omega_0$, $\upsilon_0=v_0/D_0\omega_0$, and $\Delta=D_{\mathrm{c}}/D_0$ to be four normalized (dimensionless) parameters. D_0/v_{p} is the loading time for making the spring be stretched enough to overcome the interface friction strength at $v=v_0$ or $\upsilon=\upsilon_0$. The normalized velocity, υ_{p}, of driving force is the ratio of the slipping time ω_0^{-1} to the loading time. Δ is the ratio of the maximum displacement of the slider exerted by F_0 to the characteristic slip in the friction law. The stability criteria proposed by Wang (2002) are: At low velocities, $\Delta>(\beta-\alpha)$ for the two laws; while at high velocities, $-1+\ln\Delta<\ln(\upsilon\Theta)<-1+\ln\Delta+\Delta/(\beta-\alpha)$ for the slip law and $\Delta>(\beta-\alpha)$ for the slowness law. For the slip law, the range of stable regime increases with Δ, yet decreases with increasing $\beta-\alpha$.

From the dimensionless model parameters, equation (3) becomes

$$\frac{\mathrm{d}^2U}{\mathrm{d}\tau^2}=-(U-\upsilon_{\mathrm{p}}\tau)-\left(1+\alpha\ln\frac{\upsilon}{\upsilon_0}+\beta\ln\frac{\Theta\upsilon_0}{\Delta}\right). \quad (5)$$

The normalized slip law is $\mathrm{d}\Theta/\mathrm{d}\tau=-(\Theta\upsilon/\Delta)\ln(\Theta\upsilon/\Delta)$ and the normalized slowness law is $\mathrm{d}\Theta/\mathrm{d}\tau=1-\Theta\upsilon/\Delta$. The main parameters of equation (5) are Δ, α, β, υ_0, and υ_{p}. Since υ_0 (the reference velocity) and υ_{p} (the driving velocity) are not a parameter of the frictional law, they can be individually set to be a constant. Since $\alpha-\beta$ is more important than α or β, α is fixed and β is changed, thus leading to a change of $\beta-\alpha$. Since D_0 and ω_0 are not the parameters of the friction laws, they are individually fixed to be a constant. Hence, there are only two major parameters controlling dynamical behavior of the system.

In order to conduct numerical simulations, a set of first-order ordinary differential equations associated with equation (5) is taken into account. Defining $y_1=U$, $y_2=\mathrm{d}U/\mathrm{d}\tau=\upsilon$ and $y_3=\Theta$, equation (5) becomes the following first-order differential equations:

$$\frac{\mathrm{d}y_1}{\mathrm{d}\tau}=y_2, \quad (6a)$$

$$\frac{\mathrm{d}y_2}{\mathrm{d}\tau}=\upsilon_{\mathrm{p}}\tau-y_1-\left(1+\alpha\ln\frac{y_2}{\upsilon_0}+\beta\frac{y_3\upsilon_0}{\Delta}\right) \quad (6b)$$

and

$$\frac{\mathrm{d}y_3}{\mathrm{d}\tau}=-\frac{y_2y_3}{\Delta}\ln\frac{y_2y_3}{\Delta} \quad (6c)$$

for the slip law. Equation (6c) is replaced by

$$\frac{\mathrm{d}y_3}{\mathrm{d}\tau}=1-\frac{y_2y_3}{\Delta} \quad (6d)$$

for the slowness law.

The phase portrait that is a plot of a physical quantity versus another in a dynamical system can represent dynamical behavior of the system (Thompson and Stewart, 1986). In the followings, the phase portrait is a plot of normalized velocity ($\upsilon/\upsilon_{\max}$) versus normalized displacement ($U/U_{\max}$) and will be made for different values of model parameters. U and υ are a function of Δ and $\beta-\alpha$, i.e., $\upsilon=\upsilon(\Delta,\beta-\alpha)$ and $U=U(\Delta,\beta-\alpha)$. Now, we have a two-variable problem. Nevertheless, it is not easy to demonstrate 3D simulation results. Thus, the 2D phase portraits of $v/v_{\max}$ versus $U/U_{\max}$ will be displayed, because $v/v_{\max}$ equals $\upsilon/\upsilon_{\max}$.

3 Numerical results

First, we calculate the variations of μ with v based on equation (1), together with the individual evolution laws, for four values of D_{c}, i.e., 10^{-4}, 10^{-3}, 10^{-2}, and 10^{-1} m, when $v_0=10^{-4}$ m/s. The computing technique used is the fourth-order Runge-Kutta method (Press et al, 1986). The velocity is considered to be a sine function, i.e., $v(t)=v_{\max}\sin(\omega t)$, and varies from 0 to $v_{\max}$ (10^{-3} m/s).

The value of ω is 1 s^{-1}. The time step for computations is 0.01 s. The number of divisions of velocities is 2 000, and thus the velocity unit is 5×10^{-7} m/s. Hence, the velocity at the first time step is ~5×10^{-9} m/s. The values of a and b are 0.006 and 0.009, respectively. The values of v_p are 10^{-9}, 10^{-7}, 10^{-5}, 10^{-3}, 10^{-1}, and 1 m/s. Results are shown in Figure 2 for the slip law and Figure 3 for the slowness law.

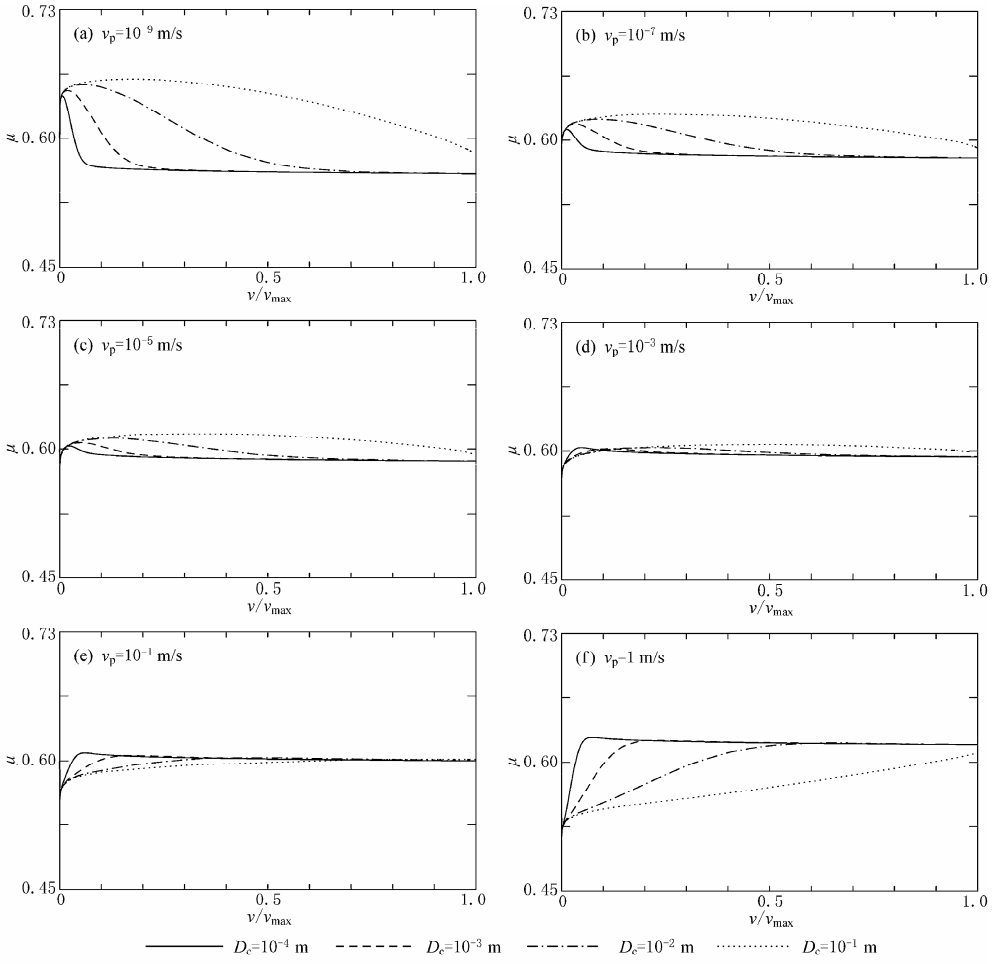

Figure 2 The variations of friction coefficient with normalized sliding velocity, v/v_{max} (v_{max}=10^{-3} m/s), for D_c=10^{-4}, 10^{-3}, 10^{-2}, and 10^{-1} m, when a=0.006 and b=0.009 for the slip law.

Based on the 1DF model, the velocity and the displacement of the slider are computed from equations (6a)–(6d) for different values of Δ and β–α using the fourth-order Runge-Kutta method. The value of α is 0.01 which is a=0.006 divided by μ_0=0.6. It is numerically intractable at υ=0. My strategy to perform the calculations at υ=0 from a value of υ related to μ_0 computed from equation (4). This value is not zero, yet smaller than υ_0. As shown in Figures 2 and 3, there is a peak in the variation of μ with v/v_{max}. When $\upsilon_p\tau\leq(\mu_0+\Psi)$, the peak behaves like a barrier which can resist motions of the slider. In order to enforce the slider to motion, a small amount of extra force must be added to increase the total force for conquering the barrier. Numerical tests show that the magnitude of the extra force is case-dependent. It cannot be a large value, because an unexpected effect could be introduced into the system due to a large extra force. A value equal to the direct effect of the friction law, i.e., a or α, is large enough to push the slider to motion and cannot make any trouble in computation. Hence, the additional force of α=0.01 is taken in simulation. This results in an initial velocity with a value of 10^{-4}, because the normalized time step is 0.01.

Numerical tests show that in a short computational time interval, the solutions can be made for a large range

of υ_p for the slip law and exist only when $\upsilon_p \geq 10^{-2}$ for the slowness law. For the slowness law, after the slider moves the driving force cannot be larger than the peak friction strength in a short computational time interval when $\upsilon_p < 10^{-2}$. Hence, a longer computational time is needed to make the slowness law work when $\upsilon_p < 10^{-2}$. On the other hand, for the slip law the driving force can be up to the peak friction strength in a short computational time for numerous values of υ_p. In order to conduct numerical simulations easily, $\upsilon_p = 10^{-2}$ is taken into account.

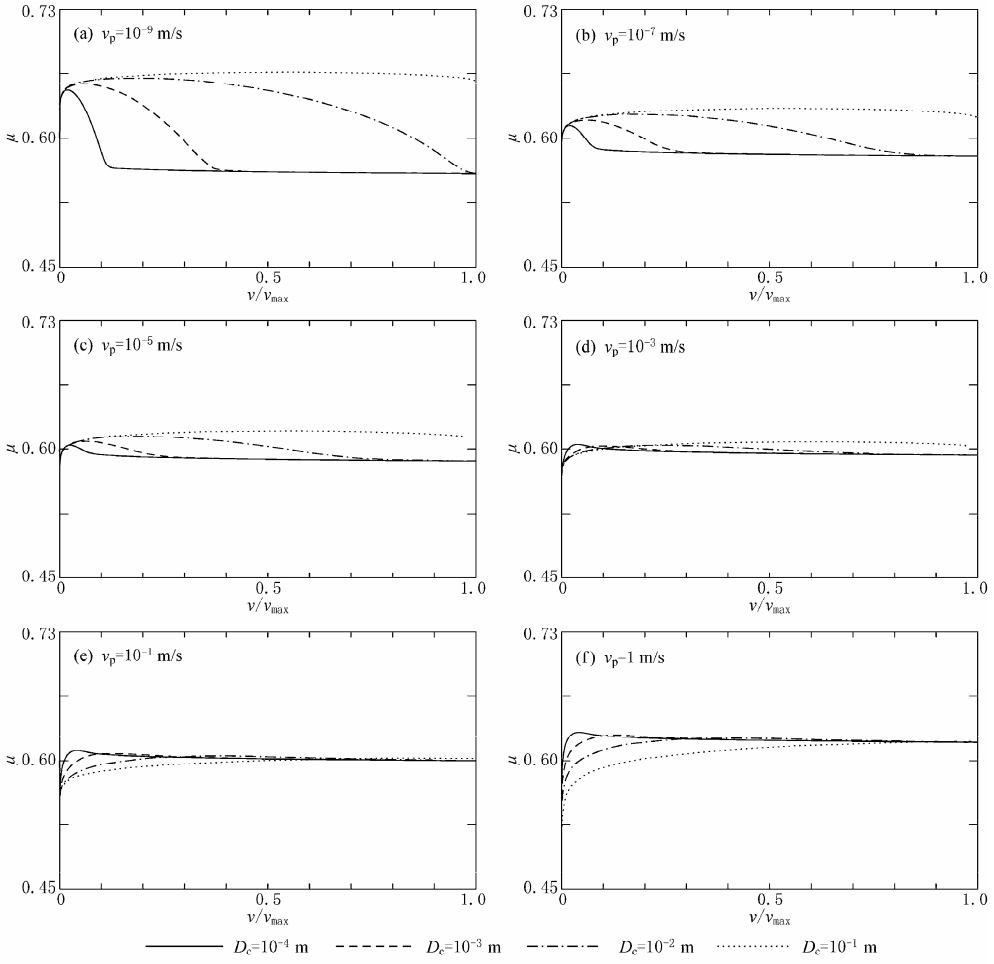

Figure 3 The variations of friction coefficient with normalized sliding velocity, v/v_{max} ($v_{max}=10^{-3}$ m/s), for $D_c=10^{-4}$, 10^{-3}, 10^{-2}, and 10^{-1} m, when a=0.006 and b=0.009 for the slowness law.

The phase portraits of v/v_{max} versus U/U_{max} are made for four values of Δ and β. The values of α, D_0, ω_0 and v_p are set to be, respectively, 0.01, 1 m, 1 s^{-1}, and 10^{-2} m/s (or $\upsilon_p=10^{-2}$). In general, $\delta\tau$ can affect stability and reliability of computed results. Numerical tests show that the simulation results for different values of $\delta\tau$ are almost equal when $\delta\tau \leq 0.01$. Hence, $\delta\tau=0.01$ is taken for saving computational time. Figure 4 shows the phase portraits for $\Delta=10^{-3}$, 10^{-2}, 10^{-1}, and 1 which are, respectively, related to $D_c=10^{-3}$, 10^{-2}, 10^{-1}, and 1 m, when D_0=1 m. Figure 5 displays the phase portraits for four values of β, i.e., 1.1×10^{-2}, 1.5×10^{-2}, 2×10^{-2}, and 6×10^{-2}. In each diagram, the solid and dashed lines represent the results for the slip law and slowness laws, respectively, and the dotted line displays the bisection line.

4 Analysis

Figure 4a shows that the solution for $\Delta=10^{-3}$ for the slowness law does not exist due to failure of stability condition. According to Wang (2002), the stability criterion for the slowness law is $\Delta > (\beta-\alpha)$ for both low and

high velocities. Thus, a stable solution exists for $\Delta>5\times10^{-3}$, yet not for $\Delta=10^{-3}<(\beta-\alpha)=5\times10^{-3}$. On the other hand, for the slip law the stability criterion of $\Delta>(\beta-\alpha)$ holds only on the quasi-static condition or at very low velocities; while at high velocities the instability condition is $-1+\ln\Delta<\ln(v\Theta)<-1+\ln\Delta+\Delta/(\beta-\alpha)$. Hence, the range of stable regime for the four values of Δ when $\beta-\alpha=5\times10^{-3}$ are (−7.90 776, −5.90 776) for $\Delta=10^{-3}$, (−5.60 517, −3.60 517) for $\Delta=10^{-2}$, (−3.30 258, +16.69 742) for $\Delta=10^{-1}$, and (−1.0, +199.0) for $\Delta=1$.

Figure 4 shows that when Δ is increased, the similarity-degree of the two phase portraits for the two friction laws increase. When $\Delta=1$ (or $D_c=1$ m), the two phase portraits are almost the same. This phenomenon still exists when $\Delta>1$. The value of D_c estimated from seismograms is usually greater than 1 m (Marone, 1998). This leads to $\Delta>1$ from observations. Hence, it is not easy to distinguish which friction law is more acceptable for controlling the earthquake rupture processes than the other when only the slip distribution of earthquake sources inferred from seismograms and/or GPS data is provided. Figure 4 displays that when $\Delta<(\beta-\alpha)$, the velocity first increases with displacement and then comes down to zero at a certain value of U/U_{max}; while when $\Delta>(\beta-\alpha)$, the velocity does not become zero and varies almost around a constant when U/U_{max} is greater than a certain value. This implicates that when U/U_{max} is greater than a certain value, the friction force cannot stop the motions of the slider and thus the slider can move steadily. This could produce a runaway event. For the 1999 Chi-Chi (Jiji), Taiwan, earthquake, Zhang et al (2003) obtained larger D_c on the northern fault plane, with larger displacements, than on the southern fault plane, with smaller displacements. Obviously, the present modeled results are consistent with observations.

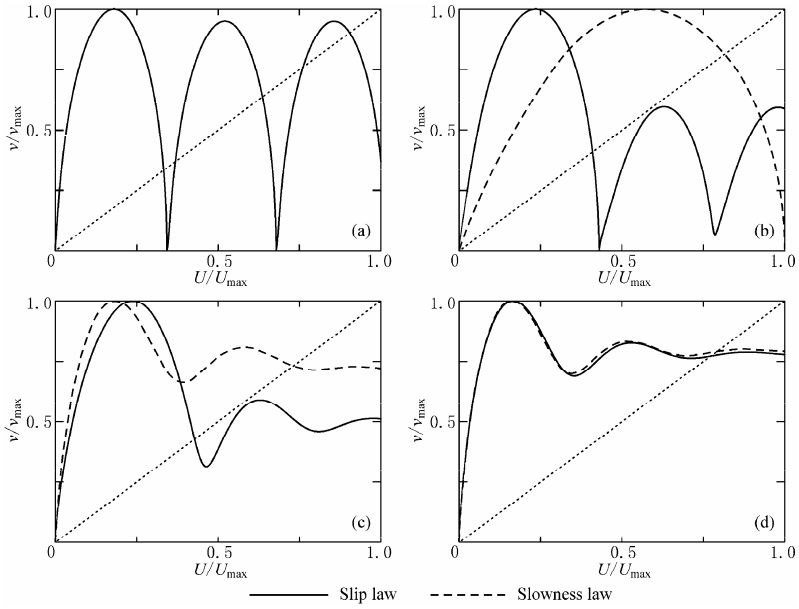

Figure 4 The phase portraits of v/v_{max} versus U/U_{max} for four values of Δ taken as 10^{-3} (a), 10^{-2} (b), 10^{-1} (c), and 1 (d), respectively. The dotted line denotes the bisection line when $\alpha=10^{-2}$, $\beta=1.5\times10^{-2}$, $\omega_0=1$ s^{-1}, $D_0=1$ m, and $v_p=10^{-2}$ m/s.

The intersection point of the bisection line with a phase portrait is called a fixed point (Thompson and Stewart, 1986). Let η be the absolute value of the slope of the tangential line at a fixed point. The stability of a fixed point is dependent upon η: stable when $\eta<1$; marginally stable when $\eta=1$; and unstable when $\eta>1$. Although the zero point (0, 0) is often a fixed point, it is a trivial one and thus not taken into account below. For the slip law, there are five fixed points as shown in Figure 4a (for $\Delta=10^{-3}$). The fixed point with the largest value of U/U_{max} is marginally stable, and others are unstable. When Δ is increased, the number of unstable fixed points decreases. When $\Delta=1$ (or $D_c=1$ m now), only the stable fixed point exists. On the other hand, there is only one stable fixed point in the three phase portraits for the slowness law.

Figure 5 shows the phase portraits for four values of β, i.e., 1.1×10^{-2}, 1.5×10^{-2}, 2×10^{-2}, and 6×10^{-2}. The

figure shows that the difference in the phase portraits between the slip law and the slowness law increases with β as well as β–α. Large β as well as large β–α, which could lead to large stress drop, cannot result in oscillations of the system with the slowness law (see Figure 5d where one of the phase portraits is coincided with the bisection line). For the slowness law, the four cases are all in the stable regime, because $\Delta=10^{-3}$ is larger than the four values of β–α. For each phase portrait with $\beta<6\times10^{-2}$ (or $\beta-\alpha<5\times10^{-2}$), the unique fixed point is stable. When $\beta=6\times10^{-2}$ (or $\beta-\alpha=5\times10^{-2}$), the phase portrait displays a linearly increasing function of velocity in terms of the displacement, thus leading to a fact that all fixed points are marginally stable. This means that large β as well as large β–α is not appropriate for the slowness law. Nevertheless, numerical results show that in the computational time interval, v_{max} and U_{max} for $\beta=6\times10^{-2}$ are both close to zero and much smaller than the related values for $\beta<6\times10^{-2}$. This indicates that small β–α is more appropriate for making the slowness law work than large β–α.

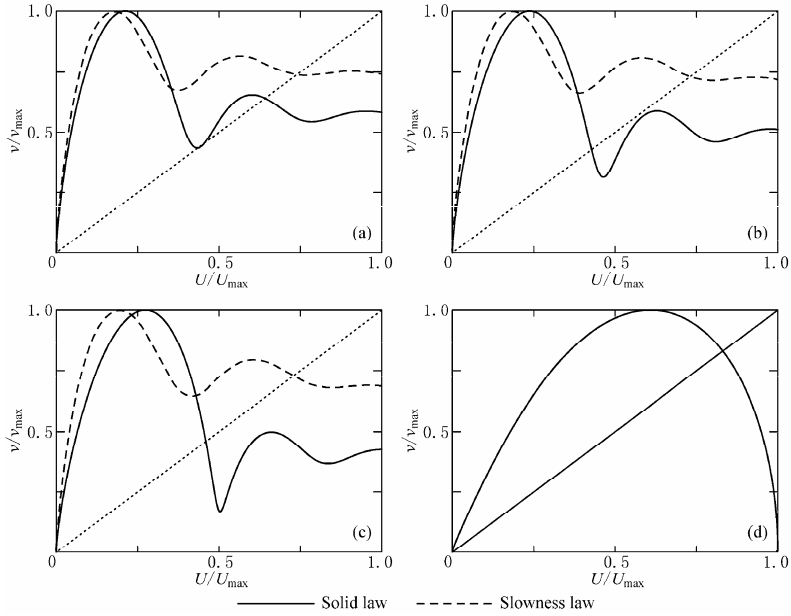

Figure 5 The phase portraits of v/v_{max} versus U/U_{max} for β taken as 1.1×10^{-2} (a), 1.5×10^{-2} (b), 2×10^{-2} (c), and 6×10^{-2} (d), respectively. The dotted line denotes the bisection line when $\alpha=10^{-2}$, $\omega_0=1$ s^{-1}, $D_0=1$ m, $D_c=10^{-1}$ m, and $v_p=10^{-2}$ m/s.

For the slip law, based on the above-mentioned the stability criterion at high velocities, the range of stable regime for the four values of β when $\alpha=10^{-2}$ and $\Delta=10^{-1}$ are: (–3.30 258, +96.69 742) for $\beta=1.1\times10^{-2}$ (or $\beta-\alpha=10^{-3}$), (–3.30 258, +16.69 742) for $\beta=1.5\times10^{-2}$ (or $\beta-\alpha=5\times10^{-3}$), (–3.30 258, +6.69 742) for $\beta=2\times10^{-2}$ (or $\beta-\alpha=10^{-2}$), and (–3.30 258, –1.30 258) for $\beta=6\times10^{-2}$ (or $\beta-\alpha=5\times10^{-2}$). The range decreases with increasing β (or with increasing β–α). The large ranges of stable regime for the four cases make solutions exist. When $\beta<6\times10^{-2}$ (or $\beta-\alpha<5\times10^{-2}$), the velocity first increases with displacement, then decreases, and finally varies around a value when U/U_{max} is greater than a certain value, which is case-dependent. Meanwhile, the number and stability of the fixed points change from one case to another. When $\beta=6\times10^{-2}$ (or $\beta-\alpha=5\times10^{-2}$), the phase portrait shows periodic motions.

5 Conclusions

Based on a one-degree-of-freedom dynamical spring-slider model, we compare two rate- and state-dependent frictional evolution laws from dynamical behavior of the slider. Numerical simulations are made from two sets of first-order differential equations, associated with two frictional evolution laws. Two (normalized) model parameters, i.e., Δ and β–α, play the main roles on controlling the solutions. On the basis of numerical simulations with given values of Δ, β, and α, for the slowness law, the solution exists when $\Delta>(\beta-\alpha)$, yet not when $\Delta<(\beta-\alpha)$. On the other hand, for the slip law the number and stability of the fixed points change from one case to another. The difference in the phase

portraits between the two friction laws decreases with increasing Δ, but increases with β–α. When Δ=1 (or D_c=1 m), the phase portraits for the two laws are almost the same, indicating that it is impossible to determine which law is more acceptable than the other just from the source rupture processes inferred from seismograms and/or GPS data, because the value of D_c estimated from seismic data is usually greater than 1 m. Nevertheless, simulation results still assume that the slip law is more appropriate of describing earthquake dynamics than the slowness law.

Acknowledgments This study was financially supported by Academia Sinica (Taipei) and Science Council (Grant NSC96-2116-M-001-012-MY3). I would like to express my sincere thanks to an anonymous reviewer and the editor for valuable comments.

References

Belardinelli M E and Belardinelli E (1996). The quasi-static approximation of the spring-slider motion. *Nonlinear Processes in Geophysics* **3**: 143–149.

Dieterich J H (1978). Time-dependent friction and the mechanics of stick-slip. *Pure Appl Geophys* **116**: 790–806.

Dieterich J H (1979). Modeling of rock friction 1. Experimental results and constitutive equations. *J Geophys Res* **84**: 2 161–2 168.

Dieterich J H (1992). Earthquake nucleation on faults with rate- and state-dependent strength. *Tectonophysics* **211**: 115–134.

Gu J-C, Rice R, Ruina A L and Tse S T (1984). Slip motion and stability of a single degree of freedom elastic system with rate and state dependent friction. *J Mech Phys Solids* **32**: 167–196.

He C, Wong T-F and Beeler N M (2003). Scaling of stress drop with recurrence interval and loading velocity for laboratory-derived fault strength relations. *J Geophys Res* **108**(B1): 2 037, doi:10.1029/2002JB001890.

Horowitz F G and Ruina A (1989). Slip patterns in a spatially homogeneous fault model. *J Geophys Res* **94**: 10 279–10 298.

Marone C (1998). Laboratory-derived friction laws and their application to seismic faulting. *Annu Rev Earth Planet Sci* **26**: 643–669.

Nakatani M (2001). Conceptual and physical clarification of rate and state friction: Frictional sliding as a thermally activated rheology. *J Geophys Res* **106**(B7): 13 347–13 380.

Perrin G, Rice J R and Zheng G (1995). Self-healing slip pulse on a frictional surface. *J Mech Phys Solids* **43**: 1 461–1 495.

Press W H, Flannery B P, Teukolsky S A and Vetterling W T (1986). *Numerical Recipes*. Cambridge Univ. Press, Cambridge, 818.

Rice J R (1983). Constitutive relations for fault slip and earthquake instabilities. *Pure Appl Geophys* **121**: 443–475.

Rice J R and Ben-zion Y (1996). Slip complexity in earthquake fault models. *Proc Natl Acad Sci*, *USA* **93**: 3 811–3 818.

Rice J R and Ruina A L (1983). Stability of steady frictional slipping. *J Appl Mech* **50**: 343–349.

Roy M and Marone C (1996). Earthquake nucleation on model faults with rate- and state-dependent friction: Effects of inertia. *J Geophys Res* **101**: 13 919–13 932.

Ruina A (1983). Slip instability and state variable friction laws. *J Geophys Res* **88**: 10 359–10 370.

Thompson J M T and Stewart H B (1986). *Nonlinear Dynamics and Chaos*. John Wiley and Sons, New York, 376.

Wang J H (2002). A dynamical study of comparing two one-variable, rate-dependent and state-dependent friction laws. *Bull Seism Soc Amer* **92**: 687–694.

Zhang W, Iwata T and Irikura K (2003). Heterogeneous distribution of the dynamic source parameters of the 1999 Chi-Chi, Taiwan, earthquake. *J Geophys Res* **108**(B5): 2 232, doi:10.1029/2002JB001889.